**Biogeosciences
Discussions**

Nitrogen cycling in the Central Arabian Sea: a model study

A. Beckmann[1] and I. Hense[2]

[1]AIONATEM, Isestrasse 84, 20149 Hamburg, Germany
[2]IHF, CEN, KlimaCampus, University of Hamburg, Grosse Elbstrasse 133, 20767 Hamburg, Germany

Correspondence to: I. Hense (inga.hense@zmaw.de)

Title Page

Abstract	Introduction
Conclusions	References
Tables	Figures

| ◄◄ | ►► |
| ◄ | ► |

Back | Close

Full Screen / Esc

Printer-friendly Version

Interactive Discussion

Abstract

We present a biogeochemical model that couples the marine nitrogen and oxygen cycles and includes euphotic, aphotic, aerobic and anaerobic processes. The model is used to investigate the mechanisms affecting nitrite and nitrogen losses in the suboxic layer of the Central Arabian Sea. In an idealized two-dimensional physical environment the model is able to reproduce the observed meridional-vertical structure of suboxic zone, secondary nitrite maximum, nitrate and oxygen. Characteristic features of vertical profiles are well represented and the modelled nitrogen transformation rates are in good agreement with observed values. The model results show that the oxygen minimum zone is not vertically homogeneous, as all suboxic processes are confined to the top 100 m of this zone. Minute differences in oxygen concentration determine the thickness of the nitrite layer. The modelled average N-loss rate in the suboxic region of the Arabian Sea is about $50\,mmol\,N\,m^{-2}\,yr^{-1}$ (about 30 times smaller than most previous estimates). The system response time scale is about 50 yr, much larger than usually assumed.

1 Introduction

The pathways of nitrogen in the ocean branch out when oxygen becomes depleted in the water column (see, e.g. reviews by Arrigo, 2005; Lam and Kuypers, 2011; Zehr and Kudela, 2011). Under low oxygen conditions the balance between the reactive nitrogen compounds, i.e. ammonium, nitrite and nitrate changes. Nitrate and nitrite are converted by bacteria to other inorganic forms of nitrogen through dissimilatory nitrate reduction to nitrite (DNRN) or ammonium (DNRA). In addition, three microbial processes eventually lead to the formation of dinitrogen gas N_2: heterotrophic and autotrophic denitrification as well as anaerobic ammonium oxidation (anammox). The former and the latter are assumed to be the main mechanisms responsible for the loss of reactive nitrogen from the system. In both denitrification processes, nitrate is reduced

to N_2. During the heterotrophic degradation process a significant amount of nitrite can be formed as an intermediate product and subsequently reduced to N_2. Autotrophic anammox bacteria reduce nitrite to oxidize ammonium while N_2 is released directly.

The Arabian Sea is one of the largest regions with low oxygen conditions (referred to as the oxygen minimum zone, OMZ) where a pronounced subsurface nitrite signal is routinely observed (see, e.g. Paulmier and Ruiz-Pino, 2009, for a recent overview). The occurrence of the so-called secondary nitrite maximum (secondary in depth not in magnitude) has often been used as direct evidence for ongoing denitrification. This has recently been called into question by Lam et al. (2011) who found indications for active dissimilatory nitrate reduction to nitrite (DNRN), which can explain the observed nitrite signal; at the same time there was hardly any N_2 production. The growth of heterotrophic denitrifiers seemed to be limited by low availability of labile organic matter; most of the N_2 (although found in low quantity) was attributed to anammox (Lam et al., 2011). Other studies suggest that heterotrophic denitrification is high and the dominant process in the presence of nitrite (Ward et al., 2009; Bulow et al., 2010). Not only the relative contributions of various pathways are unknown but also the total nitrogen loss in the Arabian Sea. Recent estimates range from about 12 (DeVries et al., 2012) to 41 (Devol et al., 2006) $Tg\,N\,yr^{-1}$. These large uncertainties and contradictory findings also raise the question of the spatial and temporal variability of the system.

So far, only few modelling studies have been carried out to address the nitrogen cycling and losses in the Arabian Sea. Anderson et al. (2007) investigate the seasonal and regional variability of denitrification with a biogeochemical nitrogen-oxygen-cycle model coupled to a three-dimensional ocean circulation model. The results are in reasonable agreement with the observational data. Their study does not, however, explicitly consider all relevant processes affecting nitrite (ammonium oxidation, nitrite oxidation, anammox). In addition, nitrate and oxygen concentrations are strongly restored to climatology below 550 m and 137 m, respectively, representing artificial sources (or sinks) of these quantities. This measure potentially masks model deficiencies due to missing processes, incorrect parameters and otherwise inaccurate oxygen and nitrate

Nitrogen cycling in the Central Arabian Sea

A. Beckmann and I. Hense

distributions. Hence, estimates of the total nitrogen loss may or may not be reliable. A different modelling approach is applied by Lam et al. (2011). Based on the observed vertical distributions of different nitrogen species, the net sources and sinks are computed from a steady state reaction-diffusion model. Since this model is applied to a single water column, three-dimensional advection and lateral diffusion are ignored. In addition, the method does not permit the identification of individual processes (anammox, denitrification, DNRN, DNRA) involved in N-cycling.

In summary, the remaining open questions concerning the nitrogen cycling in the low oxygen layers of the Arabian Sea are: What are the dominant processes that lead to the existence of a pronounced secondary nitrite maximum? What are the relevant time scales of the system? How much of the nitrogen is lost from the system?

An in-depth theoretical investigation might shed light on some of these issues. In this study, we therefore address these questions using a horizontally and vertically resolved numerical model. The biogeochemical component includes the most important aerobic or anaerobic processes (e.g. ammonium and nitrite oxidation, denitrification, anammox); it is embedded in time mean flow and turbulence fields. The model is applied in an idealized configuration representative of a typical transect through the Arabian Sea. The results are evaluated by qualitative and quantitative comparison with observations.

The paper is structured as follows: First, observed vertical profiles of different nitrogen species and oxygen are categorized into two different types (Sect. 2). The model (concept, equations and configuration) is introduced in Sect. 3. Section 4 presents the model results and their evaluation. The paper ends with a summary and conclusions (Sect. 5).

2 Observational baseline

The existence and extent of a pronounced secondary nitrite maximum in the Arabian Sea has long been demonstrated in numerous field studies, which have led to a large data base of profiles. A selection of recent casts in this region is shown in Fig. 1, where

CC BY

locations with nitrite are marked as dark and light blue dots. The occurrence of nitrite can be used to define the suboxic zone since large amounts of nitrite can accumulate only in regions where the oxygen concentrations are below a critical value (here taken as $<2\,\mu M$) so that aerobic processes cannot take place. The region with a suboxic layer therefore roughly coincides with the region of a subsurface nitrite layer (see, e.g. Naqvi, 1991).

No nitrite is found in the southern, western and far northern parts of the Arabian Sea (Fig. 1, green dots) where oxygen concentrations are too high. Typical profiles of nitrate, nitrite and oxygen at these stations (Figs 1 and 2a: profile TT043_13) are characterized by a sharp increase of nitrate below the surface mixed layer (SML), followed by a gradual increase to about $40\,mmol\,m^{-3}$ in 1500 m depth. Oxygen concentrations decrease strongly below the SML, but they remain high enough to support aerobic processes throughout the water column. Oxygen is recharged both from above (through primary production in the euphotic zone) as well as lateral and below (as a result of global ocean ventilation). Nitrite is present only in a small primary nitrite maximum at the base of the SML. The formation of the primary nitrite maximum is not fully understood; it is, however, assumed that phytoplankton is responsible for the release of nitrite due to incomplete assimilation of nitrate (Lomas and Lipschultz, 2006). Since we are mainly interested in the nitrogen pathways in the suboxic zone, we do not further consider the primary nitrite maximum.

The vertical profiles in the central and north-eastern parts of the Arabian Sea are significantly different. Light blue dots in Fig. 1 indicate profiles of the type shown in Fig. 2b (profile TT043_11). In these locations, a suboxic zone (defined by an O_2 concentration of less than $2\,\mu M$) exists and a subsurface nitrite signal is found. In many profiles, suboxic conditions occur directly below the SML. A distinct peak in nitrite with concentrations up to a few μM in about 200 m depth is typical. The nitrite maximum coincides with a strong reduction in nitrate. Summing up both reactive nitrogen species reveals a non-monotonic profile, indicative of nitrogen loss. The nitrite layer is about 100 m thick and the distributions are often symmetrical with respect to the maximum.

Nitrogen cycling in the Central Arabian Sea

A. Beckmann and
I. Hense

Title Page

Abstract | Introduction

Conclusions | References

Tables | Figures

◄ | ►

◄ | ►

Back | Close

Full Screen / Esc

Printer-friendly Version

Interactive Discussion

Nitrite profiles of this type are abundant in the center of the Arabian Sea, i.e. in the region that we call the "edge" of the suboxic zone.

The nitrite signal is even more pronounced in the north-eastern part of the Arabian Sea (dark blue dots in Figs. 1, 2c: profile TT043_7) where the top of the suboxic zone is located deeper (in about 200 m depth). The sharp increase in nitrite over a distance of only 50 m is contrasted by a quasi-linear decrease from the maximum at 250 m down to about 700 m. Again, the nitrite maximum corresponds to the nitrate minimum, affecting, however, a much larger portion of the upper water column. Profiles of nitrite at other locations within this "core" of the suboxic zone (Fig. 1, dark blue dots) all share this specific vertical asymmetry, even though in some cases the vertical shape is disturbed by lateral intrusions of water masses with different concentrations of nitrite.

The three profiles presented here are representative for our categories "outside", "edge" and "core". They have been chosen as the reference, because they originate from the same cruise and are comparatively well resolved in the vertical.

3 Model description

3.1 Basic concept

The target area for this study is the poorly ventilated, oligotrophic region of the Arabian Sea. In order to describe the pathways of nitrogen under aerobic and anaerobic conditions, a biogeochemical model is developed that combines the nitrogen and oxygen cycle. Two-dimensional (horizontal-vertical) advection and diffusion are considered through prescribed time-mean flow and diffusivity fields. External input of nitrogen (i.e. nitrogen fixation and atmospheric deposition of ammonium combined) and lateral input/output of nitrate is included. These fluxes are balanced by the loss of nitrogen through detrital sinking below the level of the nutrient (nitrate) maximum as well as due to anaerobic nitrogen loss processes (denitrification and anammox). A steady state solution is obtained, analyzed and compared with observations.

In the configuration of the physical environment, we have made use of "Occam's razor", i.e. we exclude as many complicating aspects of the physical environment as possible, as long as the main phenomenology is captured and general quantitative agreement is obtained. One of the advantages of this approach is that the relevant processes can be identified and that certain hypotheses can be ruled out. Additional details can be dealt with in later refinements.

3.2 Biogeochemical model

The biogeochemical model considers the different marine nitrogen pathways and uses stoichiometric ratios as specified in Appendix A. It uses 7 prognostic variables: phytoplankton (P), nitrate (NO_3), ammonium (NH_4), nitrite (NO_2), two detritus pools (D_L, D_R) and oxygen (O_2); for simplicity, NO_3^-, NO_2^- and NH_4^+ are called NO_3, NO_2 and NH_4, respectively. Figure 3 shows the coupled nitrogen and oxygen fluxes between the different model compartments.

The different groups of aerobic and anaerobic bacteria are not explicitly included as prognostic variables. Instead, we assume these organisms are generally abundant in their respective niches. Thus, "only" the bacterial activities, i.e. the nitrogen transformation processes are explicitly considered.

The model is a typical NPZD-type model driven by the light-limited growth of phytoplankton based on nitrate and ammonium (PPROD-A, PPROD-N) in the euphotic zone. The growth rate for ammonium based growth is assumed to be higher than nitrate based growth, because the former requires less energy (see Appendix A). The loss of phytoplankton through mortality (PMORT) is the source for the two detritus pools that differ in lability and sinking velocities. During remineralization (REMIN-L, REMIN-R) nitrogen is transferred from the detritus compartments to the ammonium pool. In low light, ammonium oxidation (AMMOX) leads to nitrite which is further oxidized (NITOX) to nitrate. Under suboxic conditions nitrate reduction to nitrite (DNRN) or ammonium (DNRA) as well as autotrophic denitrification (A-DENIT), anammox (ANAMMOX) and nitrite reduction to N_2 (NRN2) take place (to avoid confusion we have introduced the

A. Beckmann and
I. Hense

term NRN2, because the widely-used alternative "(heterotrophic) denitrification" may or may not include DNRN). The latter three processes constitute internal sink terms for nitrogen in our model. The coupled oxygen cycle considers the following processes: production through PPROD and consumption by REMIN, NITOX and AMMOX. Note that the oxygen balance is not formally closed, as water (H_2O) represents both the unlimited source for O_2 production during photosynthesis and the ultimate fate of oxygen in several aerobic and anaerobic processes. All reaction equations are given in Appendix A.

The functional dependencies and parameters to describe PPROD, PMORT and REMIN are those commonly used in ecosystem models (see, e.g. Anderson et al., 2007; Beckmann and Hense, 2007). Light and nutrient limitation of phytoplankton growth are described by the Monod kinetics with typical values for the maximum growth rate and half saturation constants. Mortality is modelled as a linear term; the mortality rate includes natural as well as grazing losses, in accordance with other model approaches (e.g. Beckmann and Hense, 2007). For the two detritus species, different remineralization rates and sinking velocities are applied, resulting in different remineralization length scales (the ratio of sinking speed and remineralization rate) of 100 m and 3000 m, respectively. This is necessary to account for the fast turnover of part of the biogenic material in the upper layers of the ocean and the simultaneous deep penetration of part of the detritus (see also Lutz et al., 2002; Lamborg et al., 2008). The refractory detritus is assumed to be resistant to denitrification; this is motivated by the fact that decomposition of refractory organic matter is hampered under anaerobic conditions (e.g. Kristensen et al., 1995).

Only few estimates of metabolic rates and half saturation constants for bacterial processes are available. The diversity of bacteria (generally and also in the ocean) is large and their metabolic pathways (e.g. anammox) and characteristics (e.g. growth rates) vary considerably. Proper description of specific processes like anammox requires the determination of all participating bacteria and the derivation of a suitably weighted average of metabolic rates and half saturation constants. This task is non-trivial and has

not been done yet. We have therefore made what we consider reasonable assumptions for all values to describe the bacterial processes: In particular, we assume that the rates of aerobic autotrophic processes are generally higher than those of aerobic heterotrophic processes and of anaerobic autotrophic processes. Aerobic and anaerobic heterotrophic processes are assumed to be of the same order of magnitude. Finally, we adopt the general notion that the rate for ANAMMOX is lower than for NRN2 (see, e.g. Dalsgaard et al., 2012, and references therein). Rate limitations for bacterial processes are again described by the Monod kinetics: AMMOX and NITOX are both suppressed under light. The heterotrophic processes DNRN, DNRA and NRN2 are limited by detritus, ANAMMOX by nitrite. In addition, aerobic processes depend on an oxygen limitation function; anaerobic processes depend on the same relationship in complementary form.

Adding sinking of detritus, advection and diffusion, the following system of prognostic equations is solved:

$$\frac{\partial P}{\partial t} = \text{PPROD-A} + \text{PPROD-N} - \text{PMORT} + \text{diff}(P) - \text{adv}(P)$$

$$\frac{\partial \text{NO}_3}{\partial t} = -\,\text{PPROD-N} + \text{NITOX} - f_N \cdot \text{DNRN} - g_N \cdot \text{DNRA} - \text{A-DENIT}$$
$$+ \text{diff}(\text{NO}_3) - \text{adv}(\text{NO}_3)$$

$$\frac{\partial \text{NH}_4}{\partial t} = -\,\text{PPROD-A} + \text{REMIN-L} + \text{REMIN-R} + f_D \cdot \text{DNRN} + h_D \cdot \text{NRN2}$$
$$+ \text{DNRA} - \text{AMMOX} - \text{ANAMMOX} + \text{diff}(\text{NH}_4) - \text{adv}(\text{NH}_4)$$

$$\frac{\partial \text{NO}_2}{\partial t} = -\,\text{NITOX} + f_N \cdot \text{DNRN} - h_N \cdot \text{NRN2} + \text{AMMOX} - \text{ANAMMOX}$$
$$+ \text{diff}(\text{NO}_2) - \text{adv}(\text{NO}_2)$$

$$\frac{\partial D_L}{\partial t} = \alpha \text{PMORT} - \text{REMIN-L} - f_D \cdot \text{DNRN} - g_D \cdot \text{DNRA} - h_D \cdot \text{NRN2}$$
$$- \text{sink}(D_L) + \text{diff}(D_L) - \text{adv}(D_L)$$

$$\frac{\partial D_R}{\partial t} = (1 - \alpha)\text{PMORT} - \text{REMIN-R} - \text{sink}(D_R) + \text{diff}(D_R) - \text{adv}(D_R)$$

$$\frac{\partial O_2}{\partial t} = q_{pN} \cdot \text{PPROD-N} + q_{pA} \cdot \text{PPROD-A} - q_r \cdot (\text{REMIN-L} + \text{REMIN-R})$$
$$- 0.5\text{NITOX} - 1.5\text{AMMOX} + \text{diff}(O_2) - \text{adv}(O_2)$$

where nitrogen (N) is the model currency for all variables except oxygen, which is given in O_2 units. In these equations, α is the allocation factor for labile detritus. The photosynthetic and respiratory quotients are q_{pN}, q_{pA} and q_r, respectively; stoichiometric factors f, g and h refer to DNRN, DNRA and NRN2, respectively, where the subscript $_N$ denotes nitrate/nitrite, while $_D$ stands for both detritus species, see also Table 1. The individual terms are:

$$\text{PPROD-N} = \mu_{\max}^N \left(\frac{I}{k_I + I} \right) \left(\frac{NO_3}{k_{NO_3} + NO_3} \right) \left(\frac{k_{NH_4}}{k_{NH_4} + NH_4} \right) P$$

$$\text{PPROD-A} = \mu_{\max}^A \left(\frac{I}{k_I + I} \right) \left(\frac{NH_4}{k_{NH_4} + NH_4} \right) P$$

$$\text{PMORT} = \gamma P$$
$$\text{REMIN-L} = \tau_{D_L} \sigma D_L$$
$$\text{REMIN-R} = \tau_{D_R} \sigma D_R$$

$$\text{AMMOX} = \epsilon_A \sigma \frac{k_I}{k_I + I} \text{NH}_4$$

$$\text{NITOX} = \epsilon_N \sigma \frac{k_I}{k_I + I} \text{NO}_2$$

$$\text{DNRN} = \delta_N (1 - \sigma) \frac{D_L}{k_{DNRN} + D_L} \text{NO}_3$$

$$\text{DNRA} = \delta_A (1 - \sigma) \frac{D_L}{k_{DNRA} + D_L} \text{NO}_3$$

$$\text{ANAMMOX} = \delta_{ANA} (1 - \sigma) \frac{\text{NO}_2}{k_{NO_2} + \text{NO}_2} \text{NH}_4$$

$$\text{NRN2} = \delta_2 (1 - \sigma) \frac{D_L}{k_{NRN2} + D_L} \text{NO}_2$$

$$\text{A-DENIT} = \nu (1 - \sigma) \text{NO}_3$$

$$\text{sink}(\phi) = w_\phi \frac{\partial \phi}{\partial z}$$

$$\text{diff}(\phi) = \frac{\partial}{\partial z} \left(A_v(z) \frac{\partial \phi}{\partial z} \right) + A_h \frac{\partial^2 \phi}{\partial y^2}$$

$$\text{adv}(\phi) = v \frac{\partial \phi}{\partial y} + w \frac{\partial \phi}{\partial z}$$

where "sink", "diff" and "adv" refer to sinking, diffusion and advection, respectively, and ϕ is a replacement character for specific prognostic variables. Central to the model is the oxygen dependence of various processes. A simple linear measure of the oxygen limitation for aerobic processes (REMIN, AMMOX and NITOX) and anaerobic processes (DNRN, DNRA, ANAMMOX, NRN2 and A-DENIT) is

$$\sigma = \frac{1}{\theta} \min(\text{O}_2, \theta)$$

where θ is the threshold value for suboxia. For a complete list of parameters see Table 1.

3.3 Model configuration

The model configuration is a two-dimensional (y-z) section through the upper ocean, thought to roughly represent a south-west–north-east transect through the Arabian Sea. The horizontal extent is 1000 km, with 20 km horizontal grid spacing. The vertical extent is limited to the upper 1500 m (roughly the depth of the nitrogen maximum where the diffusive flux vanishes, see Beckmann and Hense, 2007, 2009), the vertical grid spacing is uniformly 2 m.

The physical environment consists of a prescribed vertical profile of turbulent diffusivity, a weak lateral mixing A_h and an overturning circulation mainly confined to the upper 500 m of the fluid. Both advection and diffusion are assumed to be time-invariant (i.e. we consider seasonal time scales as unimportant for the subsurface distributions of oxygen and nitrogen species).

The vertical diffusivity profile represents (i) the surface mixed layer (SML) with high levels of mixing to produce quasi-homogeneous conditions down to its base, (ii) a barrier layer (BL) with a minimum of vertical mixing as a consequence of the strong stratification at the base of the SML and (iii) a thermocline layer (TCL) with downward increasing diffusivities (see Fig. 4 and Appendix B). The barrier layer is necessary to prevent oxygen and nitrate from excessively diffusing downward into the subsurface layers and upward into the SML, respectively. Here, the barrier layer is assumed to be located between 90 and 100 m depth throughout the model domain. This is a simplification, as the observed SML shallows northward. However, the omission of this detail does not affect the general results of this study. The functional form of the vertical mixing profile is given in Appendix B. A lateral diffusivity of $5\,m^2\,s^{-1}$ is used.

The prescribed overturning circulation is dominated by an Ekman cell in the upper 100 m, following the model results of Miyama et al. (2003). In addition, a weak upwelling circulation is prescribed in the upper 500 m, in accordance with the conceptual

idea presented in, e.g. Lee (2004). The spatial structure is shown in Fig. 4. Typical meridional velocities in upper 150 m are a few $cm s^{-1}$ (1000 km yr^{-1}), and vertical velocities of a few tens of $m yr^{-1}$. The advective transfer across the barrier layer is about 1 $m yr^{-1}$. Below 150 m depth, the maximum lateral flow is 5 km yr^{-1} and the maximum

5 upwelling velocity is 1.3 $m yr^{-1}$ in the center of the domain. The exact functional form of the streamfunction is given in the Appendix C.

The boundary conditions are of the mixed type: at the surface, a no flux condition is assumed for all variables except ammonium and oxygen. For oxygen, a surface value of 200 µM is prescribed. The external input of nitrogen is the sum of atmospheric depo-

10 sition and fixation, here treated as a combined surface flux of ammonium. The atmospheric deposition of nitrogen amounts to 5–10 mmol m^{-2} yr^{-1} (Galloway et al., 2004). Estimated values for nitrogen fixation are between 8.7 and 87 mmol m^{-2} yr^{-1} (Bange et al. (2000), computed from a total estimate for the Arabian Sea of 4.93×10^{12} m^2 horizontal area). Since today's mid-depth conditions are the result of past decades, we

15 use a conservative value for the nitrogen flux (30 mmol m^{-2} yr^{-1} in total).

At the base of the model domain (in 1500 m depth), no flux conditions for P, NO_2 and NH_4 are assumed, uniform values for nitrate (40 mmol m^{-3}) and oxygen (50 mmol m^{-3}) are specified. The lower model boundary is open for sinking detritus species. The lateral boundaries are open at outflow points, and allow for an advective and diffusive

20 influx of NO_3 and O_2 at inflow points; the external profiles for nitrate and oxygen at the southern boundary are shown in Fig. 4.

The model is initialized with vertically uniform profiles of nitrate, phytoplankton and oxygen and run to steady state (defined as a maximum pointwise imbalance of all terms of less than 0.001 mmol N m^{-2} yr^{-1}, which was reached after 3000 model yr) with a time

25 step of 100 s (for explicit time stepping). Two-dimensional advection is implemented with an upstream scheme.

4   Results and discussion

The steady state model solution provides us with two-dimensional transects and individual profiles of all state variables. We are interested in the subsurface distributions of nitrate, nitrite and oxygen, the sources and sinks of nitrite, the time scales of the system, the total N loss and the integrated nitrogen budget.

4.1   Spatial distribution of NO_3, NO_2 and O_2

The simulated oxygen, nitrite and nitrate fields are shown in Fig. 5. The oxygen distribution features concentrations of about 200 µM in the SML, an abrupt decline in the barrier layer and a minimum layer between 200 and 800 m depth (Fig. 5a). The minimum values are about 30 µM near the southern boundary, but less than 2 muM (our suboxic zone) in most of the domain. Below the minimum layer, concentrations gradually increase downward. The spatial pattern along this section is similar to the climatological fields observed in the Arabian Sea (see, e.g. WOA09, Garcia et al., 2010b). Note, however, that the oxygen values are systematically too high in the low-oxygen regions in the WOA09 climatology, as pointed out by Bianchi et al. (2012).

The corresponding nitrite distribution (Fig. 5b) coincides with the maximum horizontal extent of the suboxic zone, but is limited to its upper part. The nitrite layer thickens significantly as the distance from the southern inflow boundary increases. Maximum values reach almost 4 µM, representing a typical (albeit not extreme) nitrite signal. In general, the nitrite distribution pattern is in good agreement with the available observations from, e.g. Morrison et al. (1999).

Nitrate (Fig. 5c) is depleted throughout the SML; the subsurface nitrate distribution shows a strong vertical increase, monotonically in the south, but with an embedded subsurface minimum in the northern part of the model domain. This minimum is the result of anaerobic processes in the suboxic zone. The relatively high concentration of nitrate in the main oxicline is partly maintained by northward advection of nitrate directly

below the SML. The depth of the absolute nitrate maximum increases northward (from 850 to 1450 m), as found in the climatology (see, e.g. WOA09, Garcia et al., 2010a).

According to the classification of the observational data (see Sect. 2), the southern-most 150 km are representative of "outside" conditions, while the suboxic zone is split at km 600 into the "edge" and "core" region.

4.2 Vertical structure at selected locations

Individual profiles of NO_3, NO_2, and O_2 are shown in Fig. 6 from three different locations, representing the conditions "outside" (without any secondary nitrite maximum), in the transition zone "edge" (with a thin nitrite layer but deeper suboxic layer) and in the fully developed suboxic layer "core" (with a significant "N-deficit").

The southernmost set of profiles (Fig. 6a) is very similar to the prescribed boundary conditions, except that the upper thermocline (500–1500 m) nitrate concentrations are slightly higher. Relatively high oxygen concentrations due to lateral inflow prevent the development of a suboxic layer and therefore the production of nitrite. The other two stations ("edge" and "core") are characterized by similarly thick suboxic layers with oxygen concentrations $< 2\,\mu M$: extending from about 160 to 750–800 m (Fig. 6b, c). The nitrite signal, however, is significantly different. Nitrite is present down to a depth of 625 m at "core" compared to 275 m at the "edge" station. In both cases, nitrate within the nitrite layer is markedly reduced.

The general structure of the simulated profiles of the nitrogen species and oxygen (Fig. 6) shows striking similarity to those observed in the Arabian Sea (Fig. 2). Both magnitude and thickness of the nitrite layer compare very favorably with the observations (TT043_11 versus "edge"; TT043_7 versus "core"). In particular, the sharp increase at the top of the suboxic zone, the thin peak at "edge" and the linear decrease at "core" correspond very well to the typical profiles found in these regions.

There are, however, also systematic differences of the observed and modelled profiles: (i) there is no primary nitrite maximum at station "outside" in the model; (ii) the observed profiles are generally less smooth than the modelled ones, and the amplitude

Title Page

Abstract | Introduction

Conclusions | References

Tables | Figures

|◄ | ►|

◄ | ►

Back | Close

Full Screen / Esc

Printer-friendly Version

Interactive Discussion

of the upper nitrate maximum (referred to as the "oxicline nitrate tongue") above the suboxic zone is somewhat smaller in the model; and (iii) the sharp increase of nitrite at the top of the suboxic zone is not visible in the observations.

These differences between model and observations are related to the following factors: (i) the formation process for the primary nitrite maximum is not included in the model (this, we believe, is of little consequence for the subsurface dynamics); (ii) the prescribed circulation and mixing does not reflect regional variations of the three-dimensional flow and turbulence fields in the Arabian Sea; likewise, the surface mixed layer depth, external N input and vertical boundary conditions are assumed to be constant over the model region, while they vary in reality; (iii) the coarse resolution of the measurements (typically 50 m sampling interval) cannot resolve sharp gradients. We therefore believe that the model is more realistic in this respect.

The good correspondence of the general shape and magnitude of all three types of profiles motivates us to further investigate the nitrite dynamics within the suboxic zone.

4.3 Nitrite dynamics

The difference in the nitrite profiles between the two stations "edge" and "core" despite similarly thick suboxic layers at both stations is of particular interest. We therefore compare the modelled net production/consumption rates of nitrite as a function of depth for both stations, along with the contributions from each individual process and the oxygen concentrations (Fig. 7).

The tendency terms are significantly different from zero only at the upper and lower boundary of the nitrite layer, the magnitude and vertical structure of all individual terms differ only slightly and share the same relative proportion. In both locations the production of nitrite due to DNRN (plus a small contribution from AMMOX) occurs only in a 50 m thick layer just below the top of the suboxic layer. Consumption due to NITOX is found at the top and bottom of the nitrite layer, while NRN2 and ANAMMOX are limited to the upper 100 m. The sharp upper nitrite gradient zone at locations "edge" and "core"

(see Fig. 6) is the result of the close vertical proximity of the NITOX and DNRN peaks (Fig. 7).

Below this layer of active transformation, nitrite merely spreads diffusively downward until there is a balance with the upward diffusion of oxygen that removes the nitrite via NITOX. For "edge" this balance is reached above 300 m, because the advective and horizontal diffusive input of oxygen is still large enough to allow for some nitrite oxidation. At "core" the oxygen levels are extremely low throughout the suboxic zone, leading to accumulation of nitrite down to 600 m (see Fig. 7). Even though generally smaller than the prescribed threshold values of $\theta = 2\,\mu M$, the oxygen concentration within the suboxic zone is not uniform and negligible concentrations are necessary for the "survival" of nitrite.

The explanation for the comparably thin layer of anaerobic transformations is that the heterotrophic source and sink processes (DNRN, NRN2) require labile detritus which is available only in the upper part of the suboxic zone. Similarly, the autotrophic ANAMMOX requires ammonium which is only produced during heterotrophic (detritus-consuming) processes (remineralization, DNRN, DNRA and NRN2) and thus also restricted to the upper part of the suboxic zone.

Quantitative evaluation of the model results is possible for the "core" station, by looking at the observed rates of individual processes affecting nitrite. Rate estimates are available from five studies (see Table 3). The measurements stem from different stations, different times and are based on different methods, so that some variation is to be expected. The range of the observed values, however, is still relatively small for AMMOX (3.0–4.3 nM day^{-1}) and ANAMMOX (0.9–6.3 nM day^{-1}) but strikingly large for denitrification (from almost undetectable to 25.4 nM day^{-1}). This may be due to methodological uncertainties (see, e.g. Bulow et al., 2010; Lam and Kuypers, 2011), or due to temporal variability and/or spatial (in particular vertical) variations.

It is therefore highly encouraging that most modelled rates are of the same order of magnitude, albeit typically larger than the observations (see Table 3). This bias towards higher values in the model is not surprising because the model rates are maximum

pointwise values, while measurements at 30–200 m intervals may have missed the absolute maximum of the profile. Larger discrepancies exist for denitrification/NRN2. Note that the model rates are very similar for "core" and "edge", but that the maximum rates for station "edge" are generally higher (Table 3).

In addition to the pointwise rates, a few estimates of the vertically integrated contribution of the individual processes are available. For example, Lam et al. (2011) report a vertically integrated AMMOX rate in the core of the suboxic zone of 0.24 mmol m^{-2} day^{-1}, while the model value at station "core" is 0.29 mmol m^{-2} day^{-1}. A similar very good agreement is obtained for ANAMMOX, which is 0.1 mmol m^{-2} day^{-1} in the model versus 0.06 mmol m^{-2} day^{-1} from observations by Lam et al. (2011). Vertically integrated values for NITOX and DNRN are, however, significantly lower in the model despite higher pointwise values: while Lam et al. (2011) found a value of 7.03 mmol m^{-2} day^{-1} for NITOX and 6.91 mmol m^{-2} day^{-1} for DNRN, the model yields 1.07 mmol m^{-2} day^{-1} and 0.94 mmol m^{-2} day^{-1} for NITOX and DNRN, respectively. Although the magnitude is different, the ratio of NITOX to DNRN (slightly larger than one) is very similar in both observations and model.

An important result of this model study is that the average rates for the entire suboxic zone are significantly lower than the pointwise values (see Table 3) because active processes occur only near the top of the nitrite layer. This is in line with observations showing a strong decrease of rates with increasing depth (e.g. Bulow et al., 2010; Lam et al., 2011).

4.4 Time scales of the system

We have shown that the nitrite signal is produced by DNRN and significantly affected by vertical diffusion. Since the diffusion time scale for the suboxic zone is quite long (> 1000 yr), it can be expected that the system's response is rather slow. A sensitivity experiment was conducted to determine this response time scale. A sudden change in external nitrogen input leads to adjustments in the nitrite layer on time scales of several decades, typically 35 yr for the edge region and 50 yr in the core region. This time scale

is mainly set by DNRN, for which the model finds a minimum inverse rate of 52 yr. Note that the system response time refers to exponential changes of the inventory, i.e. after 50 yr, 64 % of the change has taken place; 90 % of the change has occurred after 2.3 exponential time scales (115 yr).

Alternatively, the model allows us to quantify the nitrite turnover time, which is often used to estimate the total nitrogen loss (see below). This time scale is calculated using the total inventory of nitrite divided by the average NLOSS rate. In our model, the average turnover time is only 14 yr and not really representative of the dynamical evolution of the system. Given the fact that the reservoir is vertically inhomogeneous and that advection and diffusion need to be considered as well, the response time scale of the system (i.e. the adjustment time scale to an external change) is a more adequate measure of the system's inertness. The apparent agreement with the estimates from Lam et al. (2011) of 49 ± 20 yr, is therefore only fortuitous, as the turnover time and system response time are conceptually different.

4.5 Nitrogen losses

In our model, reactive nitrogen is removed from the system through heterotrophic denitrification, i.e. nitrite reduction to N_2 (NRN2) and anammox (ANAMMOX), as well as autotrophic denitrification (A-DENIT). The relative contributions of these processes are 63 % ANAMMOX and 30 % NRN2; A-DENIT is rather unimportant with 7 % of the total. ANAMMOX has been found to be dominant by Lam et al. (2011) whereas other studies point towards a larger contribution from NRN2 (e.g. Ward et al., 2009). Judging from our model studies, the latter seems unlikely because an increased ANAMMOX rate and/or a reduced NRN2 rate leads to clearly unrealistic distribution patterns of nitrite, nitrate and oxygen.

Very large discrepancies exist between the nitrogen losses (NLOSS) calculated from observations (up to 2000 mmol m^{-2} yr^{-1}) and those resulting from our model (up to 60 mmol m^{-2} yr^{-1}, see Table 4). The latter are roughly 30 times smaller than those of Bulow et al. (2010) and Devol et al. (2006) which are in the range of previous estimates

(e.g. Bange et al., 2000). A similarly small annual rate of $44\,\mathrm{mmol\,m^{-2}\,yr^{-1}}$, however, can be derived from the observations by Lam et al. (2011).

To understand these differences a closer look at the two approaches used to determine nitrogen loss from observations is necessary. In the first approach pointwise measurements are extrapolated leading to a significant overestimation. Both Bulow et al. (2010) and Devol et al. (2006), for instance, extend the observed rates (obtained down to a maximum depth of 400 m) to the entire suboxic layer of 600 m thickness. As pointed out in the previous subsection, our model results indicate that source and sink processes of nitrite take place only in the upper part (50–75 m) of the suboxic zone; the rates are not uniform throughout this layer. In addition, the vertical extent of the suboxic zone is not uniformly 600 m. In the second approach, the total nitrogen loss rate is calculated from the N-deficit ΔN and a ventilation time scale (e.g. Bange et al., 2000). In simple terms, ΔN is obtained by taking the difference between the "expected" nitrate profile (derived from a statistical correlation between nitrate plus oxygen with potential temperature) and the measured nitrate concentrations. Our model allows us to calculate the N-deficit explicitly. The difference of the $NO_3 + NO_2 + NH_4$ inventory at the "outside" location and the "core" location leads to a ΔN of $11\,000\,\mathrm{mmol\,m^{-2}}$. The average N-deficit over the suboxic zone is $6000\,\mathrm{mmol\,m^{-2}}$ and therefore higher than, e.g. the estimate of $2200\,\mathrm{mmol\,m^{-2}}$ by Bange et al. (2000). This is an interesting result, which, however, should not lead to the conclusion that the modelled N loss is higher than the observational estimate. On the contrary, the time scale to create this deficit in the model is about 110 yr, i.e. almost two orders of magnitude larger than the 1–10 yr, which are usually taken as "ventilation time" for the suboxic zone. Employing such short time scales leads to a severe overestimation of the sinks.

4.6 Integrated nitrogen budget

Our final focus is the balance of nitrogen fluxes in the region with a suboxic layer. We conceptually divide the region into four layers, the surface mixed layer, the oxicline

Full Screen / Esc

Printer-friendly Version

Interactive Discussion

layer, the suboxic layer, and the oxic interior (Fig. 8). The upper two are each about 100 m thick, the suboxic layer varies in thickness. Fluxes are separated in horizontal and vertical; advective and diffusive fluxes are combined. Note that the relative proportion of "edge" and "core" regions will be different for other sections through the three-dimensional suboxic zone in the Arabian Sea; therefore, the values should not be extrapolated to the observed phenomenon. They do, however, provide a consistent picture of the main pathways of nitrogen into and out of the suboxic region.

The overall nitrogen budget of the region consists of 30 mmol m^{-2} yr^{-1} input at the surface, about the same flux to the deep ocean and a lateral net inflow that is balanced by N-losses of 54 mmol m^{-2} yr^{-1} in the suboxic zone.

The surface mixed layer receives nitrogen from external sources, and in form of nitrate from the oxicline layer. The latter is fueled by nitrogen from the divergence of lateral advection from the south (15 %), the remineralization of sinking detritus (30 %), upward diffusing oxidized nitrite (50 %) and ammonium (5 %). The detritus export from the SML is 103 mmol N m^{-2} yr^{-1}, in agreement with the 78–124 mmol N m^{-2} yr^{-1} (converted from carbon units using the Redfield ratio) found by Sarma et al. (2003) for the Eastern and Central Arabian Sea in 130 m depth.

The suboxic layer is fed by diffusive nitrate fluxes from above (24 %) and below (12 %), sinking detritus from above (46 %) and (mainly advective) lateral influx from the south (18 %). While the entering labile detritus D_L is almost completely consumed, the refractory detritus D_R passes this layer largely unaffected. Hence, more than half of the entering detritus sinks out of the suboxic zone. The main outflux of nitrogen, however, occurs at the top of the suboxic zone, through upward diffusion of nitrite and ammonium. The former is as large as the loss through denitrification and anammox.

The model results show that lateral inputs are important to maintain the balances in the suboxic zone. In particular, the "oxicline nitrate tongue", although not directly affecting the suboxic layer, is necessary to supply both the SML and the suboxic layer with nitrate.

4.7 System sensitivity

A number of experiments have been performed with modified parameters of the physical environment and the biogeochemical model to test the sensitivity of the system.

Essential elements of the physical model are the presence of a "barrier layer" of very low vertical diffusion just below the surface mixed layer (SML) to avoid extensive diffusion of oxygen to the deeper layers and at the same time to limit the upward diffusion of nitrate. Without this layer too much oxygen penetrates into the subsurface layers and prohibits the formation of a nitrite signal. Similarly, the vertical mixing in the upper thermocline layer needs to be sufficiently small (no more than 1–$2 \times 10^{-5}\,\mathrm{m^2\,s^{-1}}$) so that the suboxic zone can reach down to the observed 600–800 m. Higher mixing rates transport oxygen upward and lead to shallower nitrite layers. In addition, an overturning circulation with an inflow of nitrate below the SML as well as a general upwelling needs to be included. This is important to reproduce the "oxicline nitrate tongue" as well as the horizontal gradients in the nitrite concentrations leading to the differences in the "core" and "edge" regions of the suboxic zone. Modifying the functional dependencies for the vertical mixing coefficient and/or the overturning streamfunction, however, turned out to be qualitatively irrelevant: stronger or weaker (or even seasonally varying) wind-driven overturning with the SML does not affect the subsurface fields, nor does the depth and degree of homogeneity of the SML.

Essential elements of the biogeochemical system are the explicit inclusion of various source and sink processes of nitrite, and the consideration of (at least) two detritus species with different remineralization length scales. The former is necessary to obtain the sharp increase of nitrite at the top of the suboxic zone; the latter allows for a realistic representation of remineralization in both the oxicline and the deep ocean. The model results are not very sensitive to changes in the oxygen threshold value θ below 5. Values of 10 or more, however, lead (counter-intuitively) to a much smaller nitrite signal, because more of the nitrite produced by DNRN is oxidized within the suboxic zone by NITOX. The model results are found also insensitive to the partial allocation of

surface input into detritus compartments and/or alternative non-Redfield formulations (e.g. Anderson, 1995) of the stoichiometric relationships.

All in all, we find that model solutions with different parameter sets that share the main phenomenology with the presented ones have very similar rates and balances. Hence, we are confident that the main aspects of the system have been captured.

5 Summary and conclusions

We have developed a biogeochemical model for the marine nitrogen cycle under oxic and suboxic conditions. It has been applied in a two-dimensional configuration with prescribed circulation and mixing, and is able to reproduce the extent and magnitude of the main observed features in the Arabian Sea: the oxygen minimum zone and the nitrite signal.

According to our model results the suboxic layer of the Arabian Sea is not homogeneous, neither horizontally nor vertically. Suboxic layers (defined by a certain oxygen threshold value) of similar thickness may host thin or thick nitrite signals, depending on small changes in oxygen concentrations. The variety in vertical distributions of nitrite in the Arabian Sea can be explained by distance from oxic water columns in combination with weak upwelling.

The other reason for the non-homogeneity of the suboxic zone is the distribution of nitrite source and sink terms. NITOX as the main sink is active at the upper and lower boundaries of the nitrite layer and balanced mainly by vertical diffusion. All other processes are confined to the upper 100 m of the suboxic layer, the distance over which DNRN and NRN2 consume most of the labile detritus. The importance of labile detritus in controlling NRN2 has been also stressed by Lam et al. (2011). Their results suggest that N_2-production due to heterotrophic denitrification is strongly limited by the low availability of labile detritus in the suboxic zone of the open ocean. They conclude that the presence of nitrite is not a good indicator for active denitrification. The model results confirm this view.

An extrapolation of the model's nitrogen losses over the entire suboxic zone of the Arabian Sea (assuming an area of $1.5 \times 10^{12}\,m^2$, see Devol et al., 2006) yields a nitrogen loss of roughly $1.15\,Tg\,N\,yr^{-1}$. The majority of previous estimates range from 30 to $41\,Tg\,N\,yr^{-1}$ (Bange et al., 2000; Codispoti et al., 2001; Devol et al., 2006; Naqvi, 2008; Bulow et al., 2010). We argue that inadequate assumptions in the previously applied methods can explain this large discrepancy. First, pointwise loss rates should not be taken as representative for the entire suboxic zone. Second, the N-deficit method should not be applied with a ventilation time scale that may be adequate for the oxicline layer, but not for the layers below. The relevant system response time is closer to 100 yr than to the frequently used 1–10 yr, as proposed by, e.g. Bange et al. (2000). We therefore conclude that the nitrogen loss for the Central Arabian Sea has often been significantly overestimated. Note, however, that the main sinks of reactive nitrogen in the Arabian Sea may be located in the shelf regions (see Jensen et al., 2011), which are not part of this model study.

In this paper, we have presented a model-based view of the nitrogen cycling in the Arabian Sea suboxic zone. We realize that some of our results may be considered controversial, but would like to see them as a contribution that stimulates discussion and further observational and modelling activities.
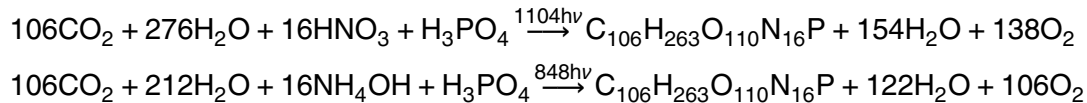
Appendix A

Marine nitrogen cycling

In the ocean, nitrogen occurs as part of organic matter, in several inorganic dissolved compounds (nutrients) and as gas. Transformations between the different nitrogen forms are biologically mediated. Some of these processes take place in the euphotic, others in the aphotic zone; some of them under aerobic, others under anaerobic conditions. Hence, the availability of light and oxygen is crucial in regulating the biological activities and therefore the nitrogen pathways. The corresponding biogeochemical

Nitrogen cycling in the Central Arabian Sea

A. Beckmann and I. Hense

Title Page

Abstract | Introduction

Conclusions | References

Tables | Figures

|◄ | ►|

◄ | ►

Back | Close

Full Screen / Esc

Printer-friendly Version

Interactive Discussion

processes are described by reaction equations that provide the stoichiometric ratios of the various constituents. The reaction equations used in our study are based on Paulmier et al. (2009) and Koeve and Kähler (2010). In addition, the equation for autotrophic denitrification has been deduced from Lam and Kuypers (2011). The stoichiometric ratios for organic matter are based on Redfield (Redfield et al., 1963). The complete set of relevant reaction equations written in the undissociated ionized form is presented below.

Primary production can take place based on nitrate or ammonium and produces oxygen. While about 1104 photons photons are needed to produce one mole of organic matter and $138\,mol\,O_2$ on nitrate basis, less photons (about 848) are required if ammonium is the source, resulting in one mole organic matter and 106 mole O_2:

$$106CO_2 + 276H_2O + 16HNO_3 + H_3PO_4 \xrightarrow{1104h\nu} C_{106}H_{263}O_{110}N_{16}P + 154H_2O + 138O_2$$

$$106CO_2 + 212H_2O + 16NH_4OH + H_3PO_4 \xrightarrow{848h\nu} C_{106}H_{263}O_{110}N_{16}P + 122H_2O + 106O_2$$

Remineralization by heterotrophic bacteria is the reverse process; this decomposition of dead organic matter (detritus) requires oxygen and releases ammonium:

$$C_{106}H_{263}O_{110}N_{16}P + 122H_2O + 106O_2 \rightarrow 106CO_2 + 212H_2O + 16NH_4OH + H_3PO_4$$
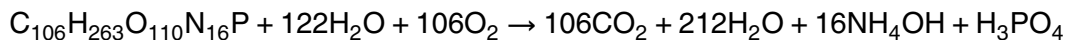
Oxidation of ammonium and nitrite take place in the aphotic (i.e. at low irradiance), oxic zone by groups of autotrophic bacteria. These two processes are sometimes combined and referred to as *nitrification*. Here they are treated separately:

$$16NH_4OH + 24O_2 \rightarrow 16HNO_2 + 32H_2O$$
$$16HNO_2 + 8O_2 \rightarrow 16HNO_3$$
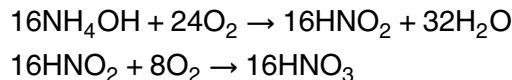
Heterotrophic nitrate reduction to nitrite/ammonium occurs only in layers with low oxygen concentrations. There are two distinct transformations: dissimilatory reduction to nitrite (DNRN), which leads to nitrite plus some ammonium and dissimilatory reduction to ammonium (DNRA) which leads to ammonium exclusively. Both processes

Nitrogen cycling in the Central Arabian Sea

A. Beckmann and I. Hense

require detritus as an energy source for the bacteria:

$$C_{106}H_{263}O_{110}N_{16}P + 212HNO_3 \rightarrow 106CO_2 + 16NH_4OH + H_3PO_4 + 212HNO_2 + 90H_2O$$
$$C_{106}H_{263}O_{110}N_{16}P + 53HNO_3 + 16H_2O \rightarrow 106CO_2 + 69NH_4OH + H_3PO_4$$

5   **N_2-production processes** lead to a loss of reactive nitrogen from the system, since dinitrogen gas (N_2) cannot be used by organisms (except by diazotrophs). The pathways to N_2 are rather complex and a number of intermediate nitrogen compounds (NO and N_2O) are produced. These specifics are ignored here, since our interest is on the main reactive nitrogen species (nitrate, nitrite and ammonium).

10   The heterotrophic process nitrite reduction to N_2 (NRN2) requires detritus and releases N_2 and ammonium:

$$3C_{106}H_{263}O_{110}N_{16}P + 424HNO_2 \rightarrow 318CO_2 + 48NH_4OH + 3H_3PO_4 + 212N_2 + 482H_2O$$
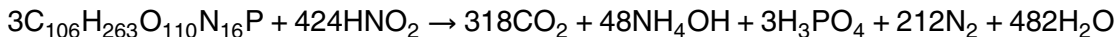
In addition to heterotrophic denitrifiers there are autotrophic bacteria that can carry out
15 denitrification; nitrate is reduced to N_2. While these bacteria have been found in the Arabian Sea, their role in the nitrogen cycle is still unclear. We include this process for completeness:

$$2HNO_3 + H_2O \rightarrow N_2 + H_2O$$

20 Finally, anaerobic ammonium oxidation (anammox) is a potentially important autotrophic process. Ammonium and nitrite are broken down by bacteria leading to the formation of N_2.

$$NH_4OH + HNO_2 \rightarrow N_2 + H_2O$$

Nitrogen cycling in the Central Arabian Sea

A. Beckmann and
I. Hense

Title Page

Abstract   Introduction

Conclusions   References

Tables   Figures
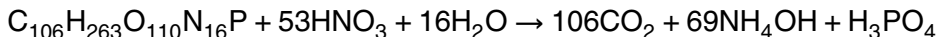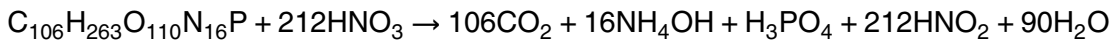
◀◀   ▶▶

◀   ▶

Back   Close

Full Screen / Esc
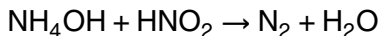
Printer-friendly Version

Interactive Discussion

Appendix B

Vertical mixing profile

The prescribed functional dependence of vertical diffusion (see Fig. 4) is given by

$$A_v = \begin{cases} A_{\text{SML}} & \text{if } z \geq z_{\text{SML}} \\ A_{\text{BL}} & \text{if } z_{\text{SML}} > z \geq z_{\text{BL}} \\ A_{\text{TCL}} + \frac{\Delta A}{2}\left(1 + \tanh\left(-\frac{(z-z_{\text{TCL}})}{h_{\text{TCL}}}\right)\right) & \text{if } z_{\text{BL}} > z \end{cases}$$

with z positively upward. The diffusivity in the surface mixed layer (down to z_{SML}) and in the barrier layer (between z_{SML} and z_{BL}) are piecewise constant, with values A_{SML} and A_{BL}, respectively. The diffusivity in the thermocline layer (TCL, centered at z_{TCL}) is gradually increasing downward. The parameter values are listed in Table 2.

Appendix C

Overturning streamfunction

The prescribed overturning streamfunction ($\Psi = \sum \Psi_i$) is composed of three parts: one for the intra-SML circulation (Ψ_1), one for the sub-SML (Ψ_2) and one for the upper ocean upwelling cell (Ψ_3). Their functional forms are:

$$\psi_1(y,z) = \Psi_1 \sin\left(\frac{\pi z}{z_{\text{SML}}}\right)\frac{1}{2}\left(1 + \tanh\left(\frac{y-y_o}{L_{\text{up}}}\right)\right)$$

$$\psi_2(z) = \Psi_2 \left[\tanh\left(\frac{z - z_{OXI}}{h_{OXI}}\right) - \tanh\left(\frac{z - z_{SRF}}{h_{OXI}}\right) \right]$$

$$\psi_3(y,z) = -\Psi_3 \, z \, \exp\left[-\left(\frac{z}{h(y)}\right)^2\right] \cos\left(\frac{\pi y}{2L_y}\right)$$

with

$$h(y) = h_o + \Delta h \left(\frac{y}{L_y}\right)^2$$

All parameter values are listed in Table 2. The prescribed overturning circulation is characterized by an Ekman cell in the upper 90 m which would have 2.5 Sv, if integrated zonally over the entire Arabian Sea. There is a northward flow beneath the SML, which is compensated by a southward flow near the surface. The interior flow consists of a closed upwelling circulation which enters from the south between 150 and 500 m depth and leaves southward in the SML.

References

Anderson, L. A.: On the hydrogen and oxygen content of marine phytoplankton, Deep-Sea Res. Pt. I, 42, 1675–1680, 1995. 13603

Anderson, T. R., Ryabchenko, V. A., Fasham, M. J. R., and Gorchakov, V. A.: Denitrification in the Arabian Sea: a 3-Decosystem modelling study, Deep-Sea Res. Pt. I, 54, 2082–2119, 2007. 13583, 13588

Arrigo, K. R.: Marine microorganisms and global nutrient cycles, Nature, 437, 349–355, 2005. 13582

Full Screen / Esc

Printer-friendly Version

Interactive Discussion

Bange, H. W., Rixen, T., Johansen, A., Siefert, R. L., Ramesh, T. R., Ittekkot, V., Hoffmann, M. R., and Andreae, M. O.: A revised nitrogen budget for the Arabian Sea, Global Biogeochem. Cy., 14, 1283–1297, 2000. 13593, 13600, 13604, 13617

Beckmann, A. and Hense, I.: Beneath the surface: characteristics of oceanic ecosystems under weak mixing conditions – a theoretical investigation, Prog. Oceanogr., 75, 771–796, 2007. 13588, 13592

Beckmann, A. and Hense, I.: A fresh look at the nutrient cycling in the oligotrophic ocean, Biogeochemistry, 96, 1–11, doi:10.1007/s10533-009-9360-6, 2009.

Bianchi, D., Dunne, J. P., Sarmiento, J. L., and Galbraith, E. D.: Data-based estimates of suboxia, denitrification, and N_2O production in the ocean and their sensitivities to dissolved O_2, Global Biogeochem. Cy., 26, GB2009, doi:10.1029/2011GB004209, 2012. 13592

Bulow, S. E., Rich, J. J., Naik, H. S., Pratihary, A. K., and Ward, B. B.: Denitrification exceeds anammox as a nitrogen loss pathway in the Arabian Sea oxygen minimum zone, Deep-Sea Res. Pt. I, 57, 384–393, 2010. 13594

Codispoti, L.: Physical oceanography and nutrients measured on water bottle samples at station TT043_07-20, doi:10.1594/PANGAEA.113068, 2003a. 13583, 13597, 13598, 13599, 13600, 13604, 13616, 13617

Codispoti, L.: Physical oceanography and nutrients measured on water bottle samples at station TT043_07-9, doi:10.1594/PANGAEA.113070, 2003b. 13619

Codispoti, L.: Physical oceanography and nutrients measured on water bottle samples at station TT043_11-1, doi:10.1594/PANGAEA.113011, 2003c. 13619

Codispoti, L.: Physical oceanography and nutrients measured on water bottle samples at station TT043_11-8, doi:10.1594/PANGAEA.113012, 2003d. 13619

Codispoti, L.: Physical oceanography and nutrients measured on water bottle samples at station TT043_13-26, doi:10.1594/PANGAEA.113017, 2003e. 13619

Codispoti, L.: Physical oceanography and nutrients measured on water bottle samples at station TT043_13-18, doi:10.1594/PANGAEA.113016, 2003f. 13619

Codispoti, L., Brandes, J. A., Christensen, J. P., Devol, A., Naqvi, S., Paerl, H. W., and Yoshinari, T.: The oceanic fixed nitrogen and nitrous oxide budgets: moving targets as we enter the anthropocene?, Scienta Marina, 65, 85–104, 2001. 13619

Dalsgaard, T., Thamdrup, B., Farías, L., and Revsbech, N. P.: Anammox and denitrification in the oxygen minimum zone of the Eastern South Pacific, Limnol. Oceanogr., 57, 1331–1346, 2012. 13604

Nitrogen cycling in the Central Arabian Sea

A. Beckmann and
I. Hense

Title Page

Abstract | Introduction

Conclusions | References

Tables | Figures

|◄ | ►|

◄ | ►

Back | Close

Full Screen / Esc

Printer-friendly Version

Interactive Discussion

Devol, A. H., Uhlenhopp, A. G., Naqvi, S. W. A., Brandes, J. A., Jayakumar, D. A., Naik, H., Gaurin, S., Codispoti, L. A., and Yoshinari, T.: Denitrification rates and excess nitrogen gas concentrations in the Arabian Sea oxygen deficient zone, Deep-Sea Res. Pt. I, 53, 1533–1547, 2006. 13589

5 DeVries, T., Deutsch, C., Primeau, F., Chang, B., and Devol, A.: Global rates of water-column denitrification derived from nitrogen gas measurements, Nat. Geosci., 5, 547–550, doi:10.1038/NGEO1515, 2012. 13583, 13599, 13600, 13604, 13616, 13617

Galloway, J. N., Dentener, F. J., Capone, D. G., Boyer, E. W., Howarth, R. W., Seitzinger, S. P., Asner, G. P., Cleveland, C., Green, P., Holland, E., Karl, D. M., Michaels, A. F., Porter, J. H.,

10 Townsend, A., and Vörösmarty, C.: Nitrogen cycles: past, present, and future, Biogeochemistry, 70, 153–226, 2004. 13583

Garcia, H. E., Locarnini, R. A., Boyer, T. P., and Antonov, J. I.: World Ocean Atlas 2009, Volume 4, Nutrients (Phosphate, Nitrate, Silicate), edited by: Levitus, S., NOAA Atlas NESDIS 70, US Government Printing Office, Washington, DC, 398, 2010a. 13593

15 Garcia, H. E., Locarnini, R. A., Boyer, T. P., Antonov, J. I., Baranova, O. K., Zweng, M. M., and Johnson, D. R.: World Ocean Atlas 2009, Volume 3, Dissolved Oxygen, Apparent Oxygen Utilization, and Oxygen Saturation, edited by: Levitus, S., NOAA Atlas NESDIS 70, US Government Printing Office, Washington, DC, 344, 2010b. 13595

Jensen, M. M., Lam, P., Revsbech, N. P., Nagel, B., Gaye, B., Jetten, M. S., and Kuypers, M. M.:

20 Intensive nitrogen loss over the Omani Shelf due to anammox coupled with dissimilatory nitrite reduction to ammonium, ISME J., 10, 1660–1670, 2011. 13594

Koeve, W. and Kähler, P.: Heterotrophic denitrification vs. autotrophic anammox – quantifying collateral effects on the oceanic carbon cycle, Biogeosciences, 7, 2327–2337, doi:10.5194/bg-7-2327-2010, 2010. 13604

25 Kristensen, E., Ahmed, S. I., and Devol, A. H.: Aerobic and anaerobic decomposition of organic matter in marine sediment: which is fastest?, Limnol. Oceanogr., 40, 1430–1437, 1995. 13605

Lam, P. and Kuypers, M. M. M.: Microbial nitrogen cycling processes in oxygen minimum zones, Ann. Rev. Mar. Sci., 3, 317–345, 2011. 13588

30 Lam, P., Jensen, M. M., Kock, A., Lettmann, K. A., Plancherel, Y., Lavik, G., Bange, H. W., and Kuypers, M. M. M.: Origin and fate of the secondary nitrite maximum in the Arabian Sea, Biogeosciences, 8, 1565–1577, doi:10.5194/bg-8-1565-2011, 2011. 13582, 13597, 13605

Title Page

Abstract | Introduction

Conclusions | References

Tables | Figures

◄ | ►|

◄ | ►

Back | Close

Full Screen / Esc

Printer-friendly Version

Interactive Discussion

Lamborg, C. H., Buesseler, K. O., Valdes, J., Bertrand, C. H., Bidigare, R., Manganini, S., Pike, S., Steinberg, D., Trull, T., and Wilson, S.: The flux of bio- and lithogenic material associated with sinking particles in the mesopelagic "twilight zone" of the Northwest and North Central Pacific Ocean, Deep-Sea Res. Pt. II, 55, 1540–1563, 2008. 13583, 13584, 13598, 13599, 13600, 13603, 13616, 13617

Lee, T.: Decadal weakening of the shallow overturning circulation in the South Indian Ocean, Geophys. Res. Lett., 31, L18305, doi:10.1029/2004GL020884, 2004. 13588

Lomas, M. W. and Lipschultz, F.: Forming the primary nitrite maximum: nitrifiers or phytoplankton?, Limnol. Oceanogr., 51, 2453–2467, 2006. 13593

Lutz, M., Dunbar, R., and Caldeira, K.: Regional variability in the vertical flux of particulate organic carbon in the ocean interior, Global Biogeochem. Cy., 16, 1037, doi:10.1029/2000GB001383, 2002. 13585

Miyama, T., McCreary, Jr., J. P., Jensen, T. G., Loschnigg, J., Godfrey, S., and Ishida, A.: Structure and dynamics of the Indian-Ocean cross-equatorial cell, Deep-Sea Res. Pt. II, 50, 2023–2047, 2003. 13588

Morrison, J. M., Codispoti, L. A., Smith, S. L., Wishner, K., Flagg, C., Gardner, W. D., Gaurin, S., Naqvi, S. W. A., Manghnani, V., Prosperie, L., and Gundersen, J. S.: The oxygen minimum zone in the Arabian Sea during 1995, Deep-Sea Res. Pt. II, 46, 1903–1931, 1999. 13592

Naqvi, S. W. A.: Geographical extent of denitrication in the Arabian Sea in relation to some physical processes, Oceanol. Acta, 14, 281–290, 1991. 13594

Naqvi, S. W. A.: The Indian Ocean, in: Nitrogen in the Marine Environment, 2nd edn., edited by: Capone, D. G., Bronk, D. A., Mulholland, M. R., and Carpenter, E. J., Elsevier, 631–704, 2008. 13585

Newell, S. E., Babbin, A. R., Jayakumar, A., and Ward, B. B.: Ammonia oxidation rates and nitrification in the Arabian Sea, Global Biogeochem. Cy., 25, GB4016, doi:10.1029/2010GB003940, 2011. 13604

Paulmier, A. and Ruiz-Pino, D.: Oxygen minimum zones (OMZs) in the modern ocean, Prog. Oceanogr., 113–128, doi:10.1016/j.pocean.2008.08.001, 2009. 13616

Paulmier, A., Kriest, I., and Oschlies, A.: Stoichiometries of remineralisation and denitrification in global biogeochemical ocean models, Biogeosciences, 6, 923–935, doi:10.5194/bg-6-923-2009, 2009. 13583

Discussion Paper | Discussion Paper | Discussion Paper | Discussion Paper |

Title Page

Abstract | Introduction

Conclusions | References

Tables | Figures

◄ | ►►

◄ | ►

Back | Close

Full Screen / Esc

Printer-friendly Version

Interactive Discussion

Redfield, A. C., Ketchum, B. H., and Richards, F. A.: The influence of organisms on the composition of sea water, in: The Sea, edited by: Hill, M. N., Wiley and Sons, New York, 26–77, 1963. 13605

Sarma, V. V. S. S., Swathi, P. S., Kumar, M. D., Prasannakumar, S., Bhattathiri, P. M. A., Madhupratap, M., Ramaswamy, V., Sarin, M. M., Gauns, M., Ramaiah, N., Sardessai, S., and de Sousa, S. N.: Carbon budget in the Eastern and Central Arabian Sea: an Indian JGOFS synthesis, Global Biogeochem. Cy., 17, 1102, doi:10.1029/2002GB001978, 2003. 13605

Ward, B. B., Devol, A. H., Rich, J. J., Chang, B. X., Bulow, S. E., Naik, H., Pratihary, A., and Jayakumar, A.: Denitrification as the dominant nitrogen loss process in the Arabian Sea, Nature, 461, 78–81, doi:10.1038/nature08276, 2009. 13601
13583, 13599, 13616

Zehr, J. P. and Kudela, R. M.: Nitrogen cycle of the open ocean: from genes to ecosystems, Ann. Rev. Mar. Sci., 3, 197–225, 2011. 13582

Title Page

Abstract · Introduction

Conclusions · References

Tables · Figures

◄ · ►

Back · Close

Full Screen / Esc

Printer-friendly Version

Interactive Discussion

Table 1. Biogeochemical model parameters.

Parameter	Description	Value	Unit
I_o	surface irradiance (PAR)	100	$W\,m^{-2}$
k_w	attenuation coefficient for water	0.05	m^{-1}
w_{D_L}	sinking velocity of labile detritus	-5	$m\,day^{-1}$
w_{D_R}	sinking velocity of refractory detritus	-15	$m\,day^{-1}$
μ_{max}^N	maximum nitrate based growth rate	0.5	day^{-1}
μ_{max}^A	maximum ammonium based growth rate	0.651	day^{-1}
k_{NO_3}	nitrate uptake half saturation constant	0.3	$mmol\,m^{-3}$
k_{NH_4}	ammonium uptake half saturation constant	0.3	$mmol\,m^{-3}$
k_{NO_2}	nitrite consumption half saturation constant	0.5	$mmol\,m^{-3}$
k_{DNRN}	detritus DNRN half saturation constant	0.05	$mmol\,m^{-3}$
k_{DNRA}	detritus DNRA half saturation constant	0.5	$mmol\,m^{-3}$
k_{NRN2}	detritus NRN2 half saturation constant	0.5	$mmol\,m^{-3}$
k_I	light harvesting half sat. const.	10	$W\,m^{-2}$
k_c	self shading coefficient	0.03	m^{-1}
γ	phytoplankton mortality	0.1	day^{-1}
α	allocation factor for labile detritus	0.75	–

Table 1. Continued.

Parameter	Description	Value	Unit
τ_D	labile detritus remineralization rate	0.05	day^{-1}
τ_R	refractory detritus remineralization rate	0.005	day^{-1}
ϵ_N	nitrite oxidation rate	0.25	day^{-1}
ϵ_A	ammonium oxidation rate	0.1	day^{-1}
δ_2	NRN2 rate	0.2	day^{-1}
δ_N	DNRN rate	0.05	day^{-1}
δ_A	DNRA rate	0.01	day^{-1}
δ_{ANA}	anammox rate	0.05	day^{-1}
ν	autotrophic nitrate reduction rate	0.000001	day^{-1}
θ	oxygen threshold	2	mmol O$_2$ m^{-3}
q_{pN}	photosynthetic quotient $\Delta O_2 : \Delta NO_3$	8.625	–
q_{pA}	photosynthetic quotient $\Delta O_2 : \Delta NH_4$	6.625	–
q_r	respiratory quotient $\Delta O_2 : \Delta NH_4$	6.625	–
f_N	DNRN factor for nitrate	212/228	–
f_D	DNRN factor for detritus	16/228	–
g_N	DNRA factor for nitrate	53/69	–
g_D	DNRA factor for detritus	16/69	–
h_N	NRN2 factor for nitrite	106/118	–
h_D	NRN2 factor for detritus	12/118	–

Discussion Paper | Discussion Paper | Discussion Paper | Discussion Paper |

Title Page

Abstract Introduction

Conclusions References

Tables Figures

◄ ►

Back Close

Full Screen / Esc

Printer-friendly Version

Interactive Discussion

Table 2. Physical model parameters.

Parameter	Description	Value	Unit
A_h	horizontal diffusivity	5	$\mathrm{m^2\,s^{-1}}$
A_{SML}	surface mixed layer diffusivity	1×10^{-2}	$\mathrm{m^2\,s^{-1}}$
A_{BL}	barrier layer diffusivity	1.5×10^{-6}	$\mathrm{m^2\,s^{-1}}$
A_{TCL}	upper thermocline layer diffusivity	1×10^{-5}	$\mathrm{m^2\,s^{-1}}$
ΔA	vertical change of thermocline layer diffusivity	1×10^{-5}	$\mathrm{m^2\,s^{-1}}$
z_{SML}	depth of surface mixed layer	-90	m
z_{BL}	depth of barrier layer base	-100	m
z_{TCL}	depth of thermocline layer center	-900	m
h_{TCL}	vertical scale of thermocline layer	200	m
Ψ_1	streamfunction amplitude	31.25×10^6	$\mathrm{m^2\,s^{-1}}$
Ψ_2	streamfunction amplitude	2×10^6	$\mathrm{m^2\,s^{-1}}$
Ψ_3	streamfunction amplitude	7600	$\mathrm{m^2\,s^{-1}}$
y_o	horizontal offset	9×10^6	m
L_{up}	horizontal scale	3×10^6	m
z_{OXI}	oxicline center	-120	m
z_{SRF}	surface current center	-10	m
h_{OXI}	vertical scale of oxicline flow	5	m
h_o	maximum vertical scale	270	m
Δh	change in vertical depth scale	135	m

Nitrogen cycling in the Central Arabian Sea

A. Beckmann and
I. Hense

Table 3. Observed and modelled rates (in $nMNday^{-1}$) of open ocean nitrite source and sink processes from the core of the suboxic region. DENIT (NRN2) refers to the loss of nitrate/nitrite to N_2 due to heterotrophic denitrification.

$(nMNday^{-1})$	AMMOX	NITOX	DNRN	ANAMMOX	DENIT (NRN2)
Devol et al. (2006)					8.2
Ward et al. (2009)[1]				~ 1	~25
Bulow et al. (2010)[2]				6.3 ± 3.2	25.4 ± 9.1
				0.9 ± 0.2	25.1 ± 5.6
Newell et al. (2011)[3]	3 ± 0.8				
	4.3 ± 0.2				
Lam et al. (2011)	3.6 ± 0.04	≤ 22[4]	29.7 ± 4.8	≤ 1.8[5]	$\ll$[6]
This model: "core"[7]	5.7	94.9	86.7	5.8	4.3
This model: "edge"[7]	7.6	116.2	121.3	6.8	4.5
This model: suboxic zone average	0.1	1.7	2.2	0.2	0.1

Comments: [1] rates determined by the exetainer method; [2] derived from two different methods: $^{15}NO_2$ or $^{46}N_2O$ for denitrification, $^{15}NO_2$ or $^{15}NH_4$ for anammox; [3] derived from two different methods: $^{15}NH_4$; $^{15}NH_4$ plus ampicillin; [4] rate might not necessarily represent NITOX, since it has been derived indirectly; [5] observed rate of N_2 production has been attributed to anammox since there was hardly any active heterotrophic denitrification (or unidentifiable pathways); [6] below the detection limit; [7] maximum values.
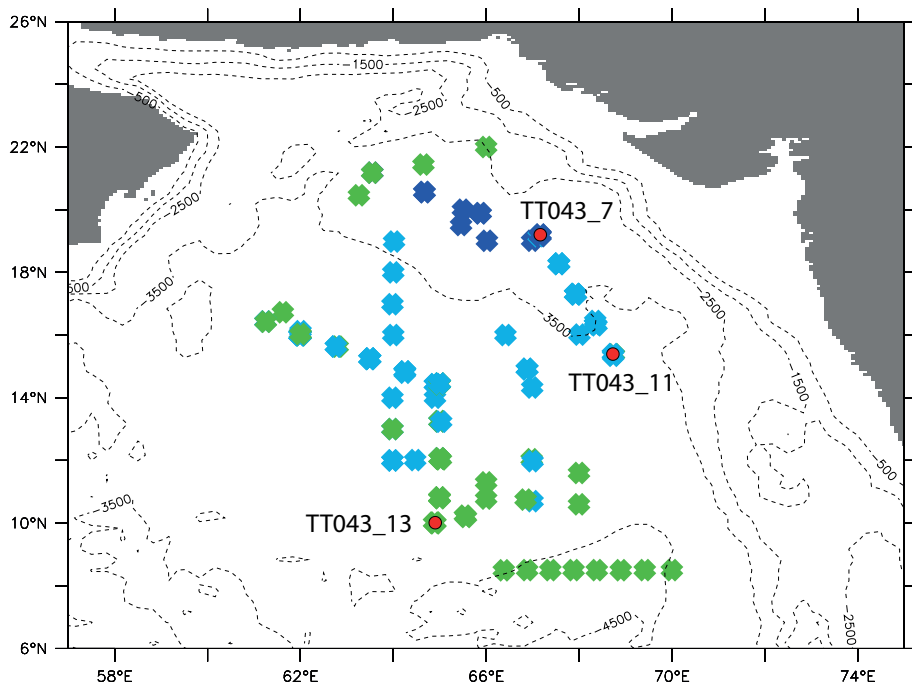
Table 4. Observed and modelled total loss of nitrogen (NLOSS) through ANAMMOX, denitrification/NRN2 and autotrophic denitrification (A-DENIT).

	NLOSS $\mathrm{mmol\,m^{-2}\,yr^{-1}}$
Bange et al. (2000)[1]	1208.8
Devol et al. (2006)[2]	1952.4
Bulow et al. (2010)[2]	1857.1
Lam et al. (2011)[3]	43.8
This model: "core"	58.3
This model: "edge"	55.9
This model: suboxic zone average	54.0

Comments: [1] published value has been divided by the given area of the suboxic zone of $1.95 \times 10^{12}\,\mathrm{m^2}$; [2] published values have been divided by the given area of the suboxic zone of $1.5 \times 10^{12}\,\mathrm{m^2}$; [3] published daily value has been multiplied by 365.25 to yield an annual rate.

Title Page

Abstract | Introduction

Conclusions | References

Tables | Figures

|◄ | ►|

◄ | ►

Back | Close

Full Screen / Esc

Printer-friendly Version

Interactive Discussion

Fig. 1. Distribution of measurements in the Arabian Sea, from the PANGAEA data base (http://www.pangaea.de). Color coding is introduced to discriminate casts with (blue) from casts without (green) a secondary nitrite maximum. Stations where the nitrite signal is penetrating deep are indicated by dark blue, those with a relatively thin nitrite layer by light blue. The locations of three typical stations with comparatively high vertical resolution (see Fig. 2) are shown as red dots. Dotted lines represent the bottom topography.

Title Page

Abstract | Introduction

Conclusions | References

Tables | Figures

◄ | ►►

◄ | ►

Back | Close

Full Screen / Esc

Printer-friendly Version

Interactive Discussion
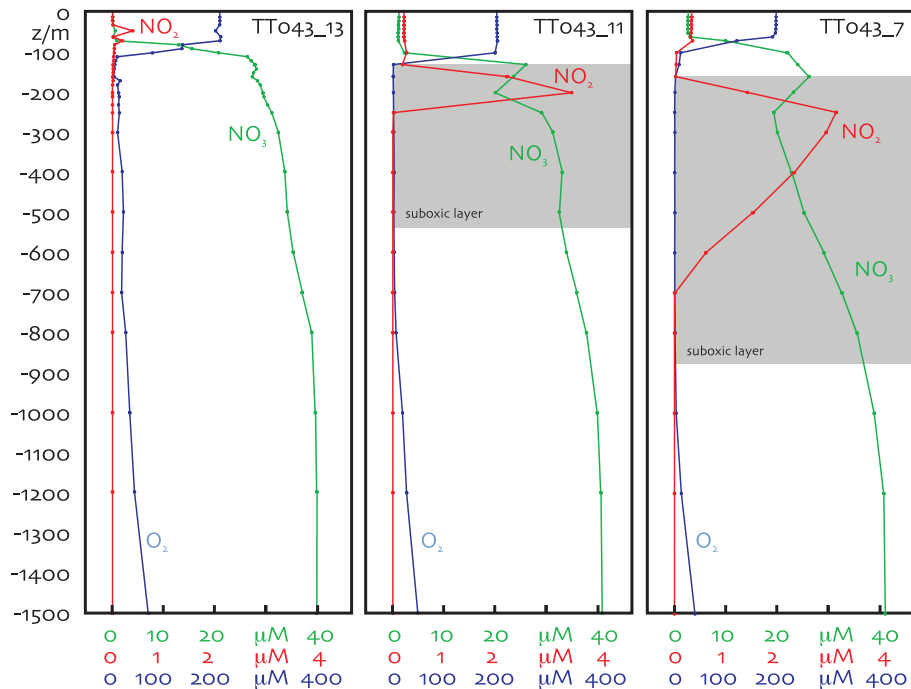
Fig. 2. Observed profiles of oxygen, nitrate and nitrite in the Arabian Sea at stations TT043_13: 10° N, 64.90° E (Codispoti, 2003e,f), TT043_11: 15.38° N, 68.75° E (Codispoti, 2003c,d), and TT043_7: 19.16° N, 67.16° E (Codispoti, 2003a,b), all from January 1995. The suboxic layer (defined by oxygen concentrations below 2 μM) is shaded in light grey.
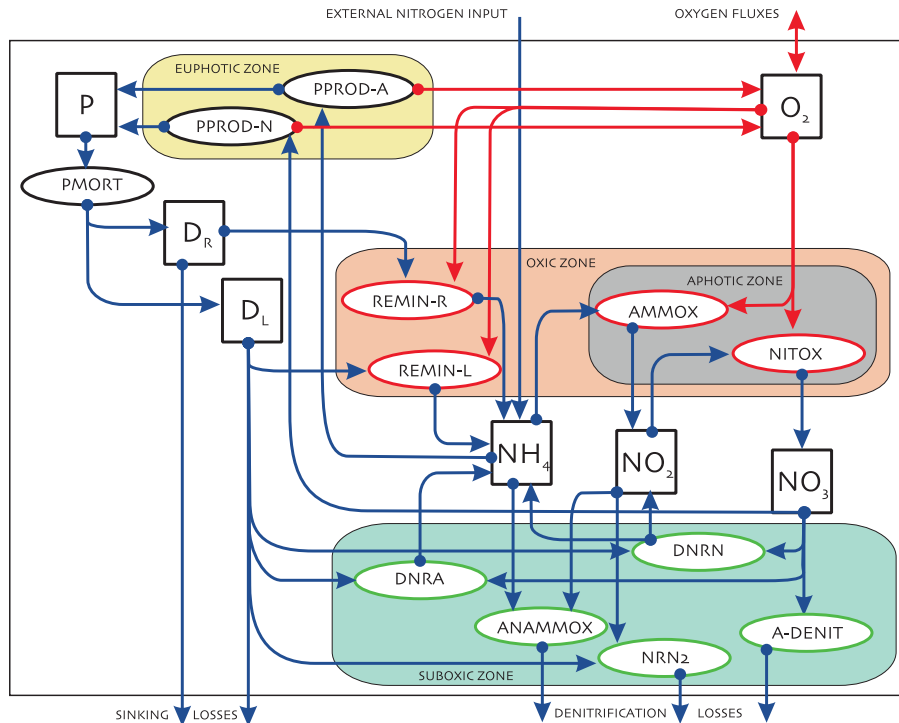
Fig. 3. Illustration of the model concept involving biogeochemical aspects of the marine nitrogen and oxygen cycles. State variables are square boxes, processes are indicated by ovals. Blue and red arrows indicate nitrogen and oxygen fluxes, respectively. Processes in the red box require oxygen, while processes in the green box occur only in case of suboxia. The yellow box contains processes that require light, while processes in the grey box occur only "in darkness".

Nitrogen cycling in the Central Arabian Sea

A. Beckmann and
I. Hense
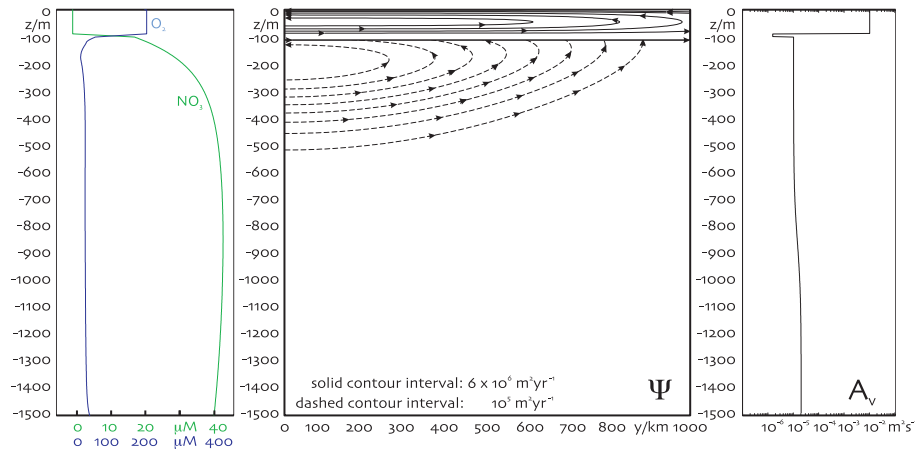
Fig. 4. The physico-chemical environment of the two-dimensional model consists of a shallow Ekman overturning circulation (center) and a prescribed vertical profile of turbulent diffusivity (right), featuring a barrier layer at the base of the mixed layer as well as a slight increase with depth within the main thermocline. The boundary conditions for nitrate and oxygen are also shown (left).
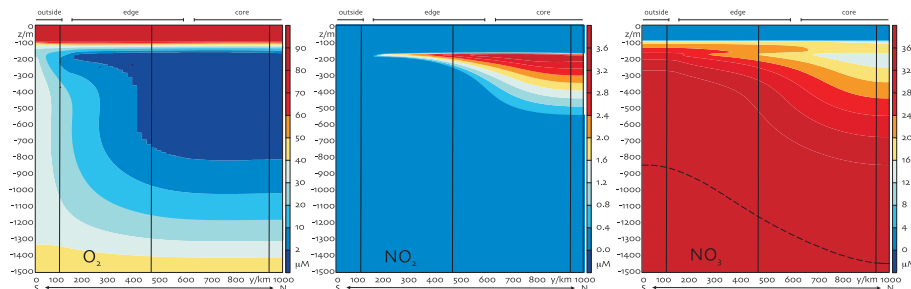
Fig. 5. Steady state distributions of oxygen, nitrite and nitrate. Vertical lines indicate the location of profiles presented in Fig. 6, representing typical cases for the core and edge as well as outside of the suboxic zone. The dashed line indicates the depth of the nitrate maximum.
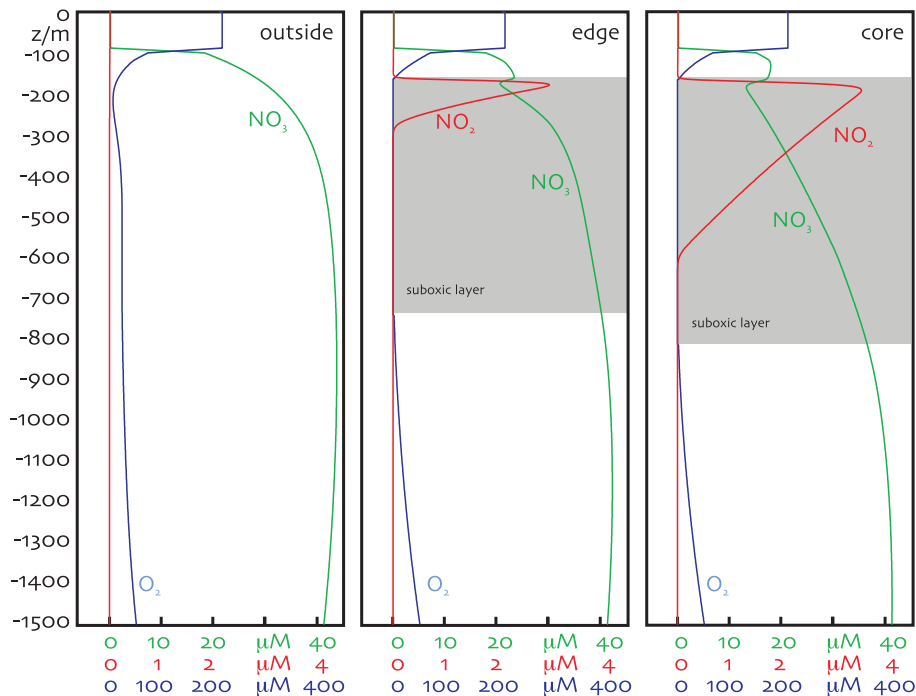
Fig. 6. Modelled profiles of oxygen, nitrate and nitrite outside, at the edge and in the core of the suboxic zone (see Fig. 5). The suboxic layer (defined by oxygen concentrations below 2 µM) is shaded in light grey.

Fig. 7. Vertical profiles of total nitrite tendencies, the oxygen concentration and the signatures of individual processes for the profiles at location "edge" and "core" in the suboxic zone. The nitrite layer is shaded in light blue.
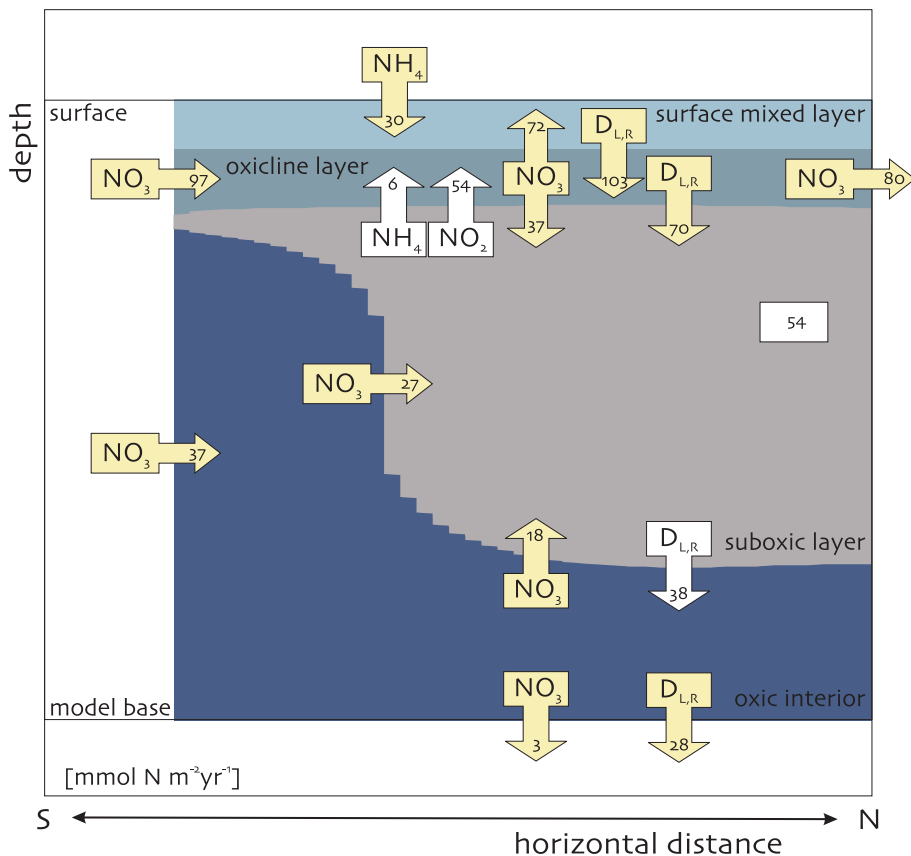
Fig. 8. Average fluxes across the boundaries of the suboxic zone (in $mmol\,N\,m^{-2}\,yr^{-1}$). Fluxes smaller than $1\,mmol\,N\,m^{-2}\,yr^{-1}$ are not shown. The sum of fluxes in the several layers may not add up to zero due to this omission and/or rounding. Losses from the suboxic layer are in white, all others in yellow.